DISCRETE-SCALE INVARIANCE AND COMPLEX DIMENSIONS

Didier SORNETTE

[a] *Laboratoire de Physique de la Matière Condensée CNRS and Université de Nice-Sophia Antipolis, Parc Valrose, 06108 Nice, France*
[b] *Department of Earth and Space Sciences and Institute of Geophysics and Planetary Physics, University of California, Los Angeles, CA 90095-1567, USA*

ELSEVIER

AMSTERDAM – LAUSANNE – NEW YORK – OXFORD – SHANNON – TOKYO

ELSEVIER

Physics Reports 297 (1998) 239–270

PHYSICS REPORTS

Discrete-scale invariance and complex dimensions

Didier Sornette[a,b]

[a] *Laboratoire de Physique de la Matière Condensée CNRS and Université de Nice-Sophia Antipolis, Parc Valrose, 06108 Nice, France*

[b] *Department of Earth and Space Sciences and Institute of Geophysics and Planetary Physics, University of California, Los Angeles, CA 90095-1567, USA*

Received July 1997; editor: I. Procaccia

Contents

Abstract

We discuss the concept of discrete-scale invariance and how it leads to complex critical exponents (or dimensions), i.e. to the log-periodic corrections to scaling. After their initial suggestion as formal solutions of renormalization group equations in the 1970s, complex exponents have been studied in the 1980s in relation to various problems of physics

PII S0370-1573(97)00076-8

embedded in hierarchical systems. Only recently has it been realized that discrete-scale invariance and its associated complex exponents may appear "spontaneously" in Euclidean systems, i.e. without the need for a pre-existing hierarchy. Examples are diffusion-limited-aggregation clusters, rupture in heterogeneous systems, earthquakes, animals (a generalization of percolation) among many other systems. We review the known mechanisms for the spontaneous generation of discrete-scale invariance and provide an extensive list of situations where complex exponents have been found. This is done in order to provide a basis for a better fundamental understanding of discrete-scale invariance. The main motivation to study discrete-scale invariance and its signatures is that it provides new insights in the underlying mechanisms of scale invariance. It may also be very interesting for prediction purposes.

PACS: 05.70.Jk; 47.53.+n; 47.54.+r; 64.60.Hr; 11.30.−j

1. Introduction

During the third century BC, Euclid and his students introduced the concept of space dimension, which can take positive integer values equal to the number of independent directions. We have to wait until the second half of the 19th century and the 20th century to witness the generalization of dimensions to fractional values. The word "fractal" is coined by Mandelbrot [1] to describe sets consisting of parts similar to the whole, and which can be described by a fractional dimension (see Ref. [2] for a compilation of the most important reprints of mathematical works leading to fractals). This generalization of the notion of a dimension from integers to real numbers reflects the conceptual jump from translational invariance to continuous-scale invariance.

The goal of this paper is to review the mathematical and physical meaning of a further generalization, wherein the dimensions or exponents are taken from the set of complex numbers.[1] We will see that this generalization captures the interesting and rich phenomenology of systems exhibiting discrete-scale invariance, a weaker form of scale-invariance symmetry, associated with log-periodic corrections to scaling.

Before explaining what is discrete-scale invariance, describing its signatures and importance and studying its mechanisms, let us present a brief historical perspective. To our knowledge, Novikov has been the first to point in 1966 that structure factors in turbulence should contain log-periodic oscillations [3]. Loosely speaking, if an unstable eddy in turbulent flow typically breaks up into two or three smaller eddies, but not into 10 or 20 eddies, then one can suspect the existence of a preferable scale factor, hence the log-periodic oscillations. The interest in log-periodic oscillations has been somewhat revived after the introduction of the renormalization group theory of critical phenomena. Indeed, the mathematical existence of such corrections has been discussed quite early in renormalization group solutions for the statistical mechanics of critical phase [4–7]. However, these log-periodic oscillations, which amount to consider complex critical exponents, were rejected for translationally invariant systems, on the (not totally correct [8]) basis that a period (even in a logarithmic scale) implies the existence of one or several characteristic scales, which is forbidden in these ergodic systems in the critical regime. Complex exponents were therefore restricted to systems with discrete renormalization groups. In the 1980s, the search for exact solution of the renormalization group led to the exploration of models put on hierarchical lattices, for which one can often obtain an exact renormalization group recursion relation. Then, by construction as we will show below, discrete-scale invariance and complex exponents and their log-periodic signature appear.

Only recently has it been realized that discrete-scale invariance and its associated complex exponents can appear spontaneously, without the need for a pre-existing hierarchical structure. It is this aspect of the domain that is the most fascinating and on which we will spend most of our time.

2. What is discrete-scale invariance (DSI)?

Let us first recall what is the concept of (continuous) scale invariance: in a nutshell, it means reproducing itself on different time or space scales. More precisely, an observable $\mathcal{O}$ which depends

[1] A further generalization to the set of quaternions (the unique non-commutative generalization of complex numbers on the set of real numbers) does not bring any new structure.

on a "control" parameter x is scale-invariant under the arbitrary change $x \to \lambda x$,[2] if there is a number $\mu(\lambda)$ such that

$$\mathcal{O}(x) = \mu\mathcal{O}(\lambda x)\,. \tag{1}$$

Eq. (1) defines a homogeneous function and is encountered in the theory of critical phenomena, in turbulence, etc. Its solution is simply a power law $\mathcal{O}(x) = Cx^{\alpha}$, with $\alpha = -\log\mu/\log\lambda$, which can be verified directly by insertion. Power laws are the hallmark of scale invariance as the ratio $\mathcal{O}(\lambda x)/\mathcal{O}(x) = \lambda^{\alpha}$ does not depend on x, i.e. the relative value of the observable at two different scales only depend on the *ratio* of the two scales.[3] This is the fundamental property that associates power laws to scale invariance, self-similarity[4] and criticality.[5]

Discrete-scale invariance (DSI) is a weaker kind of scale invariance according to which the system or the observable obeys scale invariance as defined above only for specific choices of λ (and therefore μ), which form in general an infinite but countable set of values $\lambda_1, \lambda_2, \ldots$ that can be written as $\lambda_n = \lambda^n$. λ is the fundamental scaling ratio. This property can be qualitatively seen to encode a *lacunarity* of the fractal structure [1].

Note that, since $x \to \lambda x$ and $\mathcal{O}(x) \to \mu\mathcal{O}(\lambda x)$ is equivalent to $y = \log x \to y + \log\lambda$ and $\log\mathcal{O}(y) \to \log\mathcal{O}(y + \log\lambda) + \log\mu$, a scale transformation is simply a translation of $\log x$ leading to a translation of $\mathcal{O}$. Continuous-scale invariance is thus the same as continuous translational invariance expressed on the logarithms of the variables. DSI is then seen as the restriction of the continuous translational invariance to a *discrete* translational invariance: $\log\mathcal{O}$ is simply translated when translating y by a multiple of a fundamental "unit" size $\log\lambda$. Going from continuous-scale invariance to DSI can thus be compared with (in logarithmic scales) going from the fluid state to the solid state in condensed matter physics! In other words, the symmetry group is no more the full set of translations but only those which are multiple of a fundamental discrete generator.

3. What are the signatures of DSI?

We have seen that the hallmark of scale invariance is the existence of power laws. The signature of DSI is the presence of power laws with *complex* exponents α which manifests itself in data by log-periodic corrections to scaling. To see this, consider the triadic Cantor set shown in Fig. 1. This fractal is built by a recursive process as follows. The first step consists in dividing the unit interval

[2] Here, we implicitly assume that a change of scale leads to a change of control parameter as in the renormalization group formalism. More directly, x can itself be a scale.

[3] This is only true for a function of a single parameter. Homogeneous functions of several variables take a more complex form than Eq. (1).

[4] Self-similarity is the same notion as scale invariance but is expressed in the geometrical domain, with application to fractals.

[5] Criticality refers to the state of a system which has scale-invariant properties. The critical state is usually reached by tuning a control parameter as in liquid–gas and paramagnetic–ferromagnetic-phase transitions. Many driven extended out-of-equilibrium systems seem also to exhibit a kind of dynamical criticality, that has been coined "self-organized criticality" [9].

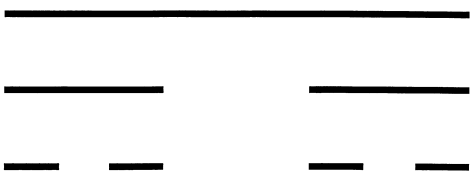

Fig. 1. Construction of the triadic Cantor set: the discrete scale invariant geometrical structure is built by a recursive process in which the first step consists in dividing the unit interval into three equal intervals of length $\frac{1}{3}$ and in deleting the central one. In the second step, the two remaining intervals of length $\frac{1}{3}$ are themselves divided into three equal intervals of length $\frac{1}{9}$ and their central intervals are deleted, thus keeping 4 intervals of length $\frac{1}{9}$, and so on.

into three equal intervals of length $\frac{1}{3}$ and in deleting the central one. In the second step, the two remaining intervals of length $\frac{1}{3}$ are themselves divided into three equal intervals of length $\frac{1}{9}$ and their central intervals are deleted, thus keeping 4 intervals of length $\frac{1}{9}$. The process is then iterated ad infinitum. It is usually stated that this triadic Cantor set has the fractal (capacity) dimension $D_0 = \log 2/\log 3$, as the number of intervals grows as 2^n while their length shrinks as 3^{-n} at the nth iteration.

It is obvious to see that, by construction, this triadic Cantor set is geometrically identical to itself *only* under magnification or coarse-graining by factors $\lambda_p = 3^p$ which are arbitrary powers of 3. If you take another magnification factor, say 1.5, you will not be able to superimpose the magnified part on the initial Cantor set. We must thus conclude that the triadic Cantor set does not possess the property of continuous-scale invariance but only that of DSI under the fundamental scaling ratio 3.

This can be quantified as follows. Call $N_x(n)$ the number of intervals found at the nth iteration of the construction. Call x the magnification factor. The original unit interval corresponds to magnification 1 by definition. Obviously, when the magnification increases by a factor 3, the number $N_x(n)$ increases by a factor 2 independent of the particular index of the iteration. The fractal dimension is defined as

$$D = \lim_{x\to\infty} \frac{\log N_x(n)}{\ln x} = \lim_{x\to 0} \frac{\ln N_x(n)}{\ln x} = \frac{\log 2}{\log 3} \approx 0.63\,. \tag{2}$$

However, the calculation of a fractal dimension usually makes use of arbitrary values of the magnification and not only those equal to $x = 3^p$ only. If we increase the magnification continuously from say $x = 3^p$ to $x = 3^{p+1}$, the numbers of intervals in all classes jump by a factor of 2 at $x = 3^p$, but then remains unchanged until $x = 3^{p+1}$, at which point they jump again by an additional factor of 2. For $3^p < x < 3^{p+1}, N_x(n)$ does not change while x increases, so the measured fractal dimension $D(x) = \ln N_x(n)/\ln x$ decreases. The value $D = 0.63$ is obtained only when x is a positive or negative power of three. For continuous values of x one has

$$N_x(n) = N_1(n)x^D P\,(\log x/\log 3)\,, \tag{3}$$

where P is a function of period unity. Now, since P is a periodic function, we can expand it as a Fourier series

$$P\left(\frac{\log x}{\log 3}\right) = \sum_{n=-\infty}^{\infty} c_n \exp\left(2n\pi \mathrm{i}\,\frac{\ln x}{\ln 3}\right). \tag{4}$$

Plugging this expansion back into Eq. (3), it appears that D is replaced by an infinity of complex values

$$D_n = D + ni\,2\pi/\log 3\,. \tag{5}$$

We now see that a proper characterization of the fractal is given by this set of *complex dimensions* which quantifies not only the asymptotic behavior of the number of fragments at a given magnification, but also its modulations at intermediate magnifications. The imaginary part of the complex dimension is directly controlled by the preferred ratio 3 under which the triadic Cantor set is exactly self-similar. Let us emphasize that DSI refers to discreteness in terms of scales, rather than discreteness in space (e.g. like discreteness of a cubic lattice approximation to a continuous medium).

If we keep only the first term in the Fourier series in Eq. (4) and insert in Eq. (3), we get

$$N_x(n) = N_1(n)x^D\,(1 + 2(c_1/c_0)\cos(2n\pi(\ln x/\ln 3)))\,, \tag{6}$$

where we have used $c_{-1} = c_1$ to ensure that $N_x(n)$ is real. Expression (Eq. (6)) shows that the imaginary part of the fractal dimension translates itself into a log-periodic modulation decorating the leading power law behavior. Notice that the period of the log-periodic modulation is simply given by the logarithm of the preferred scaling ratio. This is a fundamental result that we will retrieve in the various examples discussed below. The higher harmonics are related to the higher order dimensions.

It is in fact possible to obtain directly all these results from Eq. (1). Indeed, let us look for a solution of the form $\mathcal{O}(x) = Cx^\alpha$. Reporting in Eq. (1), we get the equation $1 = \mu\lambda^\alpha$. But 1 is nothing but $e^{i2\pi n}$, where n is an arbitrary integer. We then get

$$\alpha = -(\log\mu/\log\lambda) + i\,2\pi n/\log\lambda\,, \tag{7}$$

which has exactly the same structure as Eq. (5). The special case $n = 0$ gives the usual real power law solution corresponding to fully continuous scale invariance. In contrast, the *more general* complex solution corresponds to a possible DSI with the preferred scaling factor λ. The reason why Eq. (1) has solutions in terms of complex exponents stems from the fact that a finite rescaling has been done by the finite factor λ. In critical phenomena presenting continuous-scale invariance, Eq. (1) corresponds to the linearization, close to the fixed point, of a renormalization group equation describing the behavior of the observable under a rescaling by an arbitrary factor λ. The power law solution and its exponent α must then not depend on the specific choice of λ, especially if the rescaling is taken infinitesimal, i.e. $\lambda \to 1^+$. In the usual notation, if λ is noted $\lambda = e^{a_x\ell}$, this implies that $\mu = e^{a_\phi l}$ and $\alpha = -a_\phi/a_x$ is independent of the rescaling factor ℓ. In this case, the imaginary part in Eq. (7) drops out.

4. What is the importance and usefulness of DSI?

4.1. Existence of relevant length scales

Suppose that a given analysis of some data shows log-periodic structures. What can we get out of them? First, as we have seen, the period in log-scale of the log-periodicity is directly related to the

existence of a preferred scaling ratio. Thus, log-periodicity must immediately be seen and interpreted as the existence of a set of preferred characteristic scales forming all together a geometrical series $\ldots, \lambda^{-p}, \lambda^{-p+1}, \ldots, \lambda, \lambda^2, \ldots, \lambda^n, \ldots$. The existence of such preferred scales appears in contradiction with the notion that a critical system, exhibiting scale invariance has an infinite correlation length, hence only the microscopic ultraviolet cut-off and the large-scale infra-red cut-off (for instance the size of the system) appear as distinguishable length scales. This recovers the fact that DSI is a property different from continuous-scale invariance. In fact, it can be shown [10] that exponents are real if the renormalization group is a gradient flow, a rather common situation for systems at thermal equilibrium, but as we will see, not the only one by far. Examples when this is not the case can be found especially in random systems, out-of-equilibrium situations and irreversible growth problems. In addition to the existence of a single preferred scaling ratio and its associated log-periodicity discussed above, there can be several preferred ratios corresponding to several log-periodicities that are superimposed. This can lead to a richer behavior such as log-quasiperiodicity. Quasiperiodicity has been suggested to describe the scaling properties of diffusion-limited-aggregation clusters [11].

Log-periodic structures in the data indicate that the system and/or the underlying physical mechanisms have characteristic length scales. This is extremely interesting as this provides important constraints on the underlying physics. Indeed, simple power law behaviors are found everywhere, as seen from the explosion of the concepts of fractals, criticality and self-organized criticality [9]. For instance, the power-law distribution of earthquake energies which is known as the Gutenberg–Richter law can be obtained by many different mechanisms and a variety of models and is thus extremely limited in constraining the underlying physics. Its usefulness as a modelling constraint is even doubtful, in contradiction with the common belief held by physicists on the importance of this power law. In contrast, the presence of log-periodic features would teach us that important physical structures, that would be hidden in the fully scale-invariant description, existed.

4.2. Non-unitary field theories

In a more theoretical vein, we must notice that complex exponents do not appear in the canonical exactly solved models of critical phenomena like the square lattice Ising model or Bose Einstein condensation. This is because such models satisfy some sort of unitarity. From conformal invariance [12], it is known that the exponents of two-dimensional critical models can be measured as amplitudes of the correlation lengths in a strip geometry. Since the Ising model transfer matrix can be written in a form which is symmetric, all its eigenvalues are real, therefore all its exponents are real. The other standard example where exponents can be computed is ε expansion. However, in that context, there is an attitude, inherited from particle physics, to think mostly of Minkowski field theories. For instance, in axiomatic field theory, Euclidian field theories are defined mostly as analytic continuations of Minkowski field theories. Now complex exponents, as we have argued [8], make perfect sense for Euclidian field theories, but lead to totally ill-behaved Minkowski field theories, with exponentially diverging correlation functions. An approach based on any sort of equivalence between the two points of view is bound to discard complex exponents (as well say as complex masses). The complex exponents can thus be viewed as resulting from the breaking of equivalence (or symmetry under Wick rotation) of the Euclidian and Minkowski field theories. As it is now understood that quantum field theories are only effective theories that are essentially

critical[6] [13, 14], could there be a relation between the spectrum of observed particle masses and the characteristic scales appearing in DSI and its variants and generalizations?

4.3. Prediction

Lastly, it is important to stress the practical consequence of log-periodic structures. For prediction purposes, it is much more constrained and thus reliable to fit a part of an oscillating data than a simple power law which can be quite degenerate especially in the presence of noise. This remark has been used and is vigorously investigated in several applied domains, such as earthquakes [15–18], rupture prediction [19, 20] and financial crashes [21–23].

5. Scenarios leading to DSI

After the rather abstract description of DSI given above, we now discuss the physical mechanisms that may be found at its origin. It turns out that there is not a unique cause but several mechanisms may lead to DSI. Since DSI is a partial breaking of a continuous symmetry, this is hardly surprising as there are many ways to break down a symmetry. We describe the mechanisms that have been studied and are still under investigation. The list of mechanisms is by no means exhaustive and other mechanisms may exist. We have however tried to present a rather complete introduction to the subject.

It is essential to notice that all the mechanisms described below involve the existence of a characteristic scale (an upper and/or lower cut-off) from which the DSI can develop and cascade. In fact, for characteristic length scales forming a geometrical series to be present, it is unavoidable that they "nucleate" from either a large size or a small mesh. This remark has the following important consequences: even if the mathematical solution of a given problem contains in principle complex exponents, if there are no such cut-off scales to which the solution can "couple" to, then the log-periodicity will be absent in the physical realization of the problem. An example of this phenomenon is provided by the interface-crack stress singularity described below.

5.1. Built-in geometrical hierarchy

The most obvious situation occurs when some physical system is put on a pre-existing discrete hierarchical system, such as the Bethe lattice, or a fractal tree. Since the hierarchical system contains by construction a discrete hierarchy of scales occurring according to a geometrical series, one expects and does find complex exponents and their associated log-periodic structures. Examples are fractal dimensions of Cantor sets [24–26], percolation [27], ultrametric structures [28], wave propagation in fractal systems [29], magnetic and resistive effects on a system of wires

[6] The microscopic cut-off is the Planck scale $\sim 10^{-36}$ m while the macroscopic cut-offs (or correlation lengths) corresponding to the observed particle masses such as for the electron are of the order of 10^{-15} m. This is a situation where the correlation length is thus 10^{21} times larger than the "lattice" size, very close indeed to criticality!

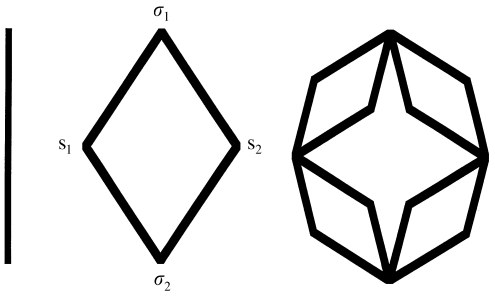

Fig. 2. Construction of the hierarchical diamond lattice used in the Potts model. This lattice is obtained by starting with a bond at magnification 1, replacing this bond by four bonds arranged in the shape of a diamond at magnification 2, and so on. The spins are placed at the sites. At a given magnification 2^p, one sees 4^p bounds, and thus $\frac{2}{3}(2+4^p)$ sites.

connected along the Sierpinski gasket [30], Ising and Potts models [31–33], fiber bundle rupture [34, 17], and sandpiles [35]. Quasiperiodic and aperiodic structures can also often be captured by a discrete renormalization group and can be expected to lead to discrete scale invariance and log-periodicity. Indeed, log-periodic corrections to scaling of the amplitude of the surface magnetization have been found for aperiodic modulations of the coupling in Ising quantum chains [36].

5.1.1. Potts model on the diamond lattice

Let us now give some details to see more clearly how physics on hierarchical systems leads to log-periodicity. As a canonical example, we treat the Potts model [37] on the diamond lattice [31]. This lattice is obtained by starting with a bond at magnification 1, replacing this bond by four bonds arranged in the shape of a diamond at magnification 2, and so on, as illustrated in Fig. 2. At a given magnification 2^p, one sees 4^p bonds, and thus $\frac{2}{3}(2+4^p)$ sites.

The spins σ_i are located at the vertices of the diamond fractal. In the same way that the lattice appears different at different scales from a geometrical point of view, one sees a different number of spins at different scales, and they will turn out to interact in a scale dependent way. For a given magnification $x = 2^p$, the spins we can see are coupled with an interaction energy

$$E = -J\sum_{\langle ij\rangle}\delta(\sigma_i\sigma_j)\,, \tag{8}$$

where J is the coupling strength, the sum is taken over nearest neighbors and the delta function equals one if arguments are equal, zero otherwise. The system is assumed at thermal equilibrium, and the spin configurations evolve randomly in time and space in response to thermal fluctuations with a probability proportional to the Boltzmann factor $\mathrm{e}^{-\beta E}$, where β is the inverse of the temperature. The partition function Z at a given magnification $x = 2^p$ is

$$Z_p = \sum_{\{\sigma\}}\mathrm{e}^{-\beta E}\,,$$

where the sum is taken over all possible spin configurations which can be seen at that scale. We do not compute Z_p completely, but first perform a partial summation over the spins seen at one scale and which are coupled only to two other spins. This is how, in this particular example, one can

carry out the program of the renormalization group by solving a succession of problems at different scales. Let us isolate a particular diamond, call σ_1,σ_2 the spins at the extremities and s_1,s_2 the spins in between as in Fig. 2. The contribution of this diamond to $e^{-\beta E}$ is

$$K^{\delta(\sigma_1,s_1)+\delta(\sigma_2,s_1)+\delta(\sigma_1,s_2)+\delta(\sigma_2,s_2)},$$

where we have defined $K = e^{\beta J}$. Since s_1, s_2 enter only in this particular product, we can perform summation over them first when we compute Z_p. The final result depends on whether σ_1 and σ_2 are equal or different:

$$\sum_{s_1,s_2} K^{\delta(\sigma_1,s_1)+\delta(\sigma_2,s_1)+\delta(\sigma_1,s_2)+\delta(\sigma_2,s_2)} = \begin{cases} (2K+Q-2)^2, & \sigma_1 \neq \sigma_2\,, \quad (9) \\ (K^2+Q-1)^2, & \sigma_1 = \sigma_2\,, \quad (10) \end{cases}$$

so we can write

$$\sum_{s_1,s_2} K^{\delta(\sigma_1,s_1)+\delta(\sigma_2,s_1)+\delta(\sigma_1,s_2)+\delta(\sigma_2,s_2)} = \begin{cases} (2K+Q-2)^2\left[1+\left(\dfrac{(K^2+Q-1)^2}{(2K+Q-2)^2}-1\right)\delta(\sigma_1,\sigma_2)\right] \\ (2K+Q-2)^2 K'^{\delta(\sigma_1,\sigma_2)}, \end{cases} \quad (11)$$

where we used the identity

$$K'^{\delta(\sigma_1,\sigma_2)} = 1 + (K' - 1)\delta(\sigma_1,\sigma_2)\,, \quad (12)$$

and we set

$$K' \equiv \left(\frac{K^2+Q-1}{2K+Q-2}\right)^2. \quad (13)$$

If we perform this partial resummation in each of the four diamonds, we obtain exactly the system at a lower magnification $x = 2^{p-1}$. We see therefore that the interaction of spins transforms very simply when the lattice is magnified: at any scale, only nearest-neighbor spins are coupled, with a scale dependent coupling determined recursively through the *renormalization group map*

$$K_{p-1} = \left(\frac{K_p^2+Q-1}{2K_p+Q-2}\right)^2 \equiv \phi(K_p)\,. \quad (14)$$

The spins which are "integrated out" by going from one magnification to the next simply contribute an overall numerical factor to the partition function, which is equal to the factor $(2K+Q-2)^2$ per edge of Eq. (12). Indeed, integrating out the spins s_1 and s_2 leaves only σ_1 and σ_2 whose interaction weight is by definition $K'^{\delta(\sigma_1,\sigma_2)}$, where K' represents the effective interaction weight at this lower magnification 2^{p-1}. The additional numerical factor shows that the partition function is not exactly invariant with the rescaling but transforms according to

$$Z_p(K) = Z_{p-1}[\phi(K)](2K+Q-2)^{2\cdot 4^p}\,, \quad (15)$$

since there are 4^p bonds at magnification 2^p. Now the free energy per spin, which is defined as the logarithm of the partition function per bond, reads

$$f_p(K) = \frac{1}{4^{p+1}} \ln Z_p(K)\,.$$

From Eq. (15), we deduce the following:

$$f_p(K) = g(K) + \tfrac{1}{4} f_{p-1}(K'), \tag{16}$$

where

$$g(K) = \tfrac{1}{2} \ln (2K + Q - 2). \tag{17}$$

For an infinite fractal, the free energy for microscopic coupling K satisfies therefore

$$f(K) = g(K) + \frac{1}{\mu} f(K'), \tag{18}$$

where $\mu = 4$. This explicit calculation makes clear the origin of the scaling for the free energy: the interaction weights remain of the same functional form at each (discrete) level of magnification, up to a multiplicative factor which accounts for the degrees of freedom "left-over" when integrating from one magnification to the next. This is the physical origin of the function g in Eq. (18).

5.1.2. Fixed points, stable phases and critical point

Consider the map $K' = \phi(K)$ Eq. (14). It exhibits three fixed points (defined by $K' = K = \phi(K)$) located at $K = 1$, $K = \infty$, $K = K_c$ where K_c is easily determined numerically, for instance $K_c \approx 3.38$ for $Q = 2$, $K_c \approx 2.62$ for $Q = 1$. That $K = 1$ and $K = \infty$ are fixed points is obvious. The former corresponds to totally uncoupled spins, the latter to spins which are forced to have the same value. In both cases, the dynamics disappears completely, and one gets back to a purely geometrical problem. Observe that these two fixed points are attractive. This means that if we start with some coupling say $K > K_c$ deep down in the system, that is for very large magnifications, when one diminishes the magnification to look at the system at macroscopic scales, spins appear almost always parallel, and therefore are more and more correlated as one reduces magnification. Similarly if we start with $K < K_c$ spins are less and less correlated as one reduces magnification. The condition $K > K_c$ together with the definition $K = e^{\beta J}$ implies $\beta > \beta_c$, i.e. corresponds to the low-temperature regime dominated by the energy. The physical meaning of the attraction of the renormalization group flow to the fixed point $K = \infty$, i.e. zero temperature, means that the macroscopic state of the spins is ferromagnetic with a macroscopic organization where a majority of spins have the same value. Similarly, the condition $K < K_c$ implies $\beta < \beta_c$, i.e. corresponds to the high-temperature regime dominated by the entropy or thermal agitation. The physical meaning of the attraction of the renormalization group flow to the fixed point $K = 0$, i.e. infinite temperature, means that the macroscopic state is completely random with zero macroscopic magnetization.

The intermediate fixed point K_c, which in contrast is repulsive, plays a completely different and very special role. It does not describe a stable thermodynamic phase but rather the transition from one phase to another. The repulsive nature of the renormalization group map flow means that this transition occurs for a very special value of the control parameter (the temperature or the coupling weight $K = K_c$). Indeed, if we have spins interacting with a coupling strength right at K_c at microscopic scales, then even by reducing the magnification we still see spins interacting with a coupling strength right at K_c! This is also a point where spins must have an infinite correlation length (otherwise it would decrease to zero as magnification is reduced, corresponding to a different effective interaction): by definition it is a *critical* point.

Close to K_c we can linearize the renormalization group transformation

$$K' - K_c \approx \lambda(K - K_c)\,, \tag{19}$$

where $\lambda = \mathrm{d}\phi/\mathrm{d}K|_{K_c} > 1$. For couplings close enough to the critical point, we now see that as we increase magnification, the change in coupling becomes also very simple; only, it is not the coupling that gets renormalized by a multiplicative factor, but the distance to K_c.

Eq. (18) together with Eq. (19) provides an explicit realization of the postulated functional form (Eq. (1)) (up to the non-singular term g), where the coupling parameter K (in fact $K - K_c$) plays the role of the control parameter x.

5.1.3. Singularities and log-periodic corrections

The renormalization group Eqs. (14) and (18) can be solved for the free energy by

$$f(K) = \sum_{n=0}^{\infty} \frac{1}{\mu^n} g[\phi^{(n)}(K)]\,, \tag{20}$$

where $\phi^{(n)}$ is the nth iterate of the transformation ϕ (e.g. $\phi^{(2)}(x) = \phi[\phi(x)]$). Now it is easy to show [129] that the sum (Eq. (20)) is *singular* at $K = K_c$. This stems from the fact that K_c is an unstable fixed point, so the derivative of ϕ at K_c is $\lambda > 1$. Therefore, if we consider the kth derivative of f in Eq. (20) it is determined by a series whose generic term behaves as $(\lambda^k/\mu)^n$ which is greater than 1 for k large enough, so this series diverges. In other words, high enough derivatives of f are infinite at K_c. Very generally, this implies that close to K_c one has

$$f(K) \propto (K - K_c)^m\,, \tag{21}$$

where m is called a *critical exponent*. For instance, if $0 < m < 1$, the derivative of f diverges at the critical point. Plugging this back in Eq. (18), we see that, since g is regular at K_c as can be checked easily from Eq. (17), we can substitute it in Eq. (18) and recover the leading critical behavior and derive m solely from the equation $(K - K_c)^m = (1/\mu)[\lambda(K - K_c)]^m$ involving only the singular part, with the flow map which has been linearized in the vicinity of the critical point. Therefore, the exponent satisfies $\lambda^m = \mu$, an equation that we have already encountered and whose general solution is given by

$$m_n = \frac{\ln \mu}{\ln \lambda} + n\mathrm{i}\frac{2\pi}{\ln \lambda}\,. \tag{22}$$

To get expression (Eq. (22)), we have again used the identity $\mathrm{e}^{\mathrm{i}2\pi n} = 1$. We see that because there is discrete-scale invariance (namely Eq. (18) holds which relates the free energy only at two different scales in the ratio 2), nothing forces m to actually be a real number. In complete analogy with the case of complex fractal dimension, a critical phenomenon on a fractal exhibits *complex critical exponents*. Of course f is real, so the most general form of f close to the critical point should be

$$f(K) \approx (K - K_c)^m \left\{ a_0 + \sum_{n>0} a_n \cos\left[2\pi n \Omega \ln(K - K_c) + \Psi_n\right] \right\}, \tag{23}$$

where

$$m = \ln \mu/\ln \lambda\,, \quad \Omega = 1/\ln \lambda\,, \tag{24}$$

hence exhibiting the log-periodic corrections. Derrida et al. [31] have studied this example more quantitatively and find that the amplitude of the log-periodic oscillations are of the order of 10^{-4} times the leading behavior. This is thus a small effect. In contrast, the examples below exhibit a much stronger amplitude of the log-periodic corrections to scaling, that can reach 10% or more.

5.1.4. Related examples in programming and number theory

Log-periodicity, many of which are of a fractal nature, are found in the solutions of algorithms based on a recursive *divide-and-conquer* strategy [38] such as heapsort, mergesort, Karatsuba's multiprecision multiplication, discrete Fourier transform, binomial queues, sorting networks, etc. For instance, it is well-known that the worst-time cost measured in the number of comparisons that are required for sorting n elements by the MergeSort procedure is given by $n \log_2 n$ to leading order. It is less known that the first subleading term is $nP(\log_2 n)$, where P is periodic [38].

Reducing a problem to number theory is like striping it down to its sheer fundamentals. In this vein, arithmetic functions related to the number representation systems exhibit various log-periodicities. For instance, the total number of ones in the binary representations of the first n integers is $\frac{1}{2}n \log_2 n + nF(\log_2 n)$, where F is a fractal function, continuous, periodic and nowhere differentiable [39].

5.2. Diffusion is anisotropic quenched random lattices

In this scenario, the DSI hierarchy is constructed dynamically in a random walk process due to intermittent encounters with slow regions [40]. Consider a random walker jumping from site to site. Bonds between sites are of two types: (i) directed ones on which the walker surely goes from his site to the next on his right ("diode" situation); (ii) two-way bonds characterized by a rate u (resp. v) to jump to the neighboring site on his right (resp. left). The fraction of two-way bonds is $1 - p$ and the fraction of directed bonds is p. We construct a *frozen* random lattice by choosing a given configuration of randomly distributed mixtures of the two-bond species according to their respective average concentration p and $1 - p$. The exact solution of this problem has been given in [40] and shows very clearly nice log-periodic oscillations in the dependence of $\langle x^2 \rangle$ as a function of time, as seen in Fig. 3.

We now present a simple scaling argument [17] which recovers the exact results. To do so, we assume $u/v \ll 1 - p \ll 1$. We are thus is a situation where most bonds are directed and dilute clusters of two-way bonds are present. In addition, the two bonds are strongly impeding the progress of the walker as the forward rate to the right is much smaller than the backward rate to the left.

In this situation, the random walker progresses at constant velocity to the right as long as it encounters only diode bonds and gets partially trapped when it encounters two-way bonds. To see how DSI is spontaneously generated, we estimate the typical number of jumps τ_k needed for the random walker to pass k adjacent two-way bonds, i.e. a connected cluster of k two-way bonds. In the limit $u/v \ll 1$, $\tau_k \sim (v/u)^k$.[7] Using the fact that the average separation between k-tuples of

[7] and not $\tau_k \sim k\, v/u$. This is due to the fact that the walker goes back and forth many times before escaping from the cluster of size k.

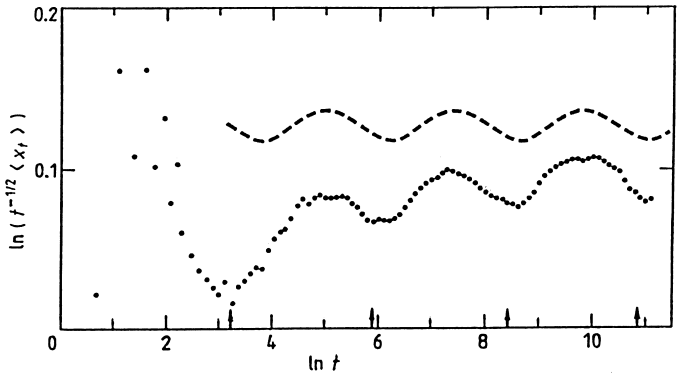

Fig. 3. $\langle x^2(t)\rangle/t^{2\nu_R}$, where $\nu_R = \log(1-p)/\log(u/v)$ is the real part of Eq. (26) as a function of $\ln t$. The averaging has been performed over different realizations of the random walk (taken from Ref. [40]).

two-way bonds is approximately $(1-p)^{-k}$, if $u/v \ll (1-p)$, the typical number of jumps needed for the random walker to go beyond the first k-tuple of consecutive two-way values is completely dominated by τ_k. One thus expects the rate as a function of the number of jumps to exhibit local minima at $\tau = \tau_k$: these are the jump-numbers time scales. The second part of the scaling argument consists in recognizing that the random walker has to cover a typical distance from the origin to encounter the first k-tuple of consecutive 'two-way' values, of the order of $(1-p)^{-k}$. In the limit where $u/v \ll (1-p) \ll 1$, we can thus write the approximate renormalization group equation

$$x(\tau) \approx (1-p)x(\lambda\tau) + g(\tau)\,, \tag{25}$$

where we have set $\lambda \equiv v/u$ and $g(\tau)$ is some regular function taking into account various local effects that correct the main scaling. Notice the similarity with Eq. (18). Because this renormalization group equation can be written only at scales which are powers of λ, we are back to the situation discussed before. We see in particular that $x \sim \tau^{\nu}$ with

$$\nu = \frac{\log(1-p)}{\log(u/v)} + \mathrm{i}\frac{2\pi n}{\log(u/v)}. \tag{26}$$

This result for the exponent ν turns out to be exact. Furthermore, the range of parameters over which this holds is much larger than suggested by this intuitive argument. More precisely, as soon as $u/v < (1-p)$, one finds $x(\tau) \sim \tau^{\nu}\ P(\log\tau/\log(v/u))$, where $\nu = \log(1-p)/\log(u/v)$ and P is a periodic function of unit period. This prediction is remarkably well-confirmed by numerical simulations and recovers the exact calculation of [40]. This is shown in Fig. 3.

This mechanism for generating log-periodic oscillations makes use of an interplay between dynamics and quenched randomness leading to a regime where the dynamics is highly intermittent. The presence of the discrete lattice and the mesh size is essential. Similar intermittent amplification processes have been studied in Refs. [41, 42]. Log-periodicity found in the solutions of boolean delay equations [43, 44] stems from a similar mechanism.

This should not give the impression that log-periodicity is an artifact of 1D systems. Also, random walks with a fixed bias direction on randomly diluted lattices in three dimensions with densities far above the percolation threshold show log-periodic oscillations in $x(\tau)$ versus τ [145]. The physical mechanism is similar, in which dead ends play the role of 'two-way' bonds.

5.3. Cascade of ultraviolet instabilities: Growth processes and rupture

5.3.1. Log-periodicity in the geometrical properties

Numerical analysis of large diffusion-limited aggregates have uncovered a *discrete* scaling invariance in their inner structure, which can be quantified by the introduction of a set of *complex* fractal dimensions [11]. The values of the complex fractal dimensions can be predicted *quantitatively* from a renormalization group approach using the quasiperiodic mapping found in Refs. [45–47].

A theoretical investigation of a simplified model of DLA, the needle problem, which is also of direct application to crack growths has been done to identify the underlying physical mechanism [48]. Based on perturbative analysis and some exact results from the hodograph method in the 2D conformal plane, we find that the two basic ingredients leading to DSI are the short-wavelength Mullins–Sekerka instability[8] and the strong screening of competing needles. The basic simple picture that emerges is that *non-linear* interactions between the unstable modes of the set of needles lead to a succession of period doubling, the next sub-harmonic catching up and eventually screening the leading unstable mode. The succession of these period doubling explains the existence of discrete-scale invariance in these systems. We thus think that short-wavelength instabilities of the Mullins–Sekerka type supplemented by a strong screening effect provides a general scenario for the *spontaneous* formation of log-periodic structures. This scenario provides, in addition, an explanation for the observation of a preferred scaling ratio close to 2.

Numerical simulations of the needle problem, using various growth rules (DLA, angle screening, η-model, crack approximation) on systems containing up to 5000 needles confirm clearly the proposed scenario, as shown in Fig. 4. The density of needles as a function of the distance to the base presents clear evidence of log-periodic modulations of the leading algebraic decay. Geological data on joints competing in their growth in a similar fashion also exhibit approximately the log-periodic structure [48, 49]. Refs. [50, 51] present further data on joints which, in our eyes, exhibit clearly log-periodicity, even if the authors were not aware of the concept. Various previous investigation of the growth of arrays of cracks have shown the log-periodic structures, even if the authors neither point it out nor explained the mechanism [52–54].

What we learn by comparing these different systems, with various growth rules, is that the spontaneous formation of DSI seems robust with respect to significant modifications. The improvement of our understanding of DLA resides on the identification of a spontaneous generation of an approximately discrete cascade of Mullins–Sekerka instabilities from small scales to large scales. This discreteness results from a cascade of mode selections by a non-linear non-perturbative

[8] The Mullins–Sekerka instability is nothing other than the "lightning rod effect" well-known in electrostatics, according to which large curvature concentrates the gradient of the potential field. Here, the growth velocity is proportional to the gradient of the concentration field.

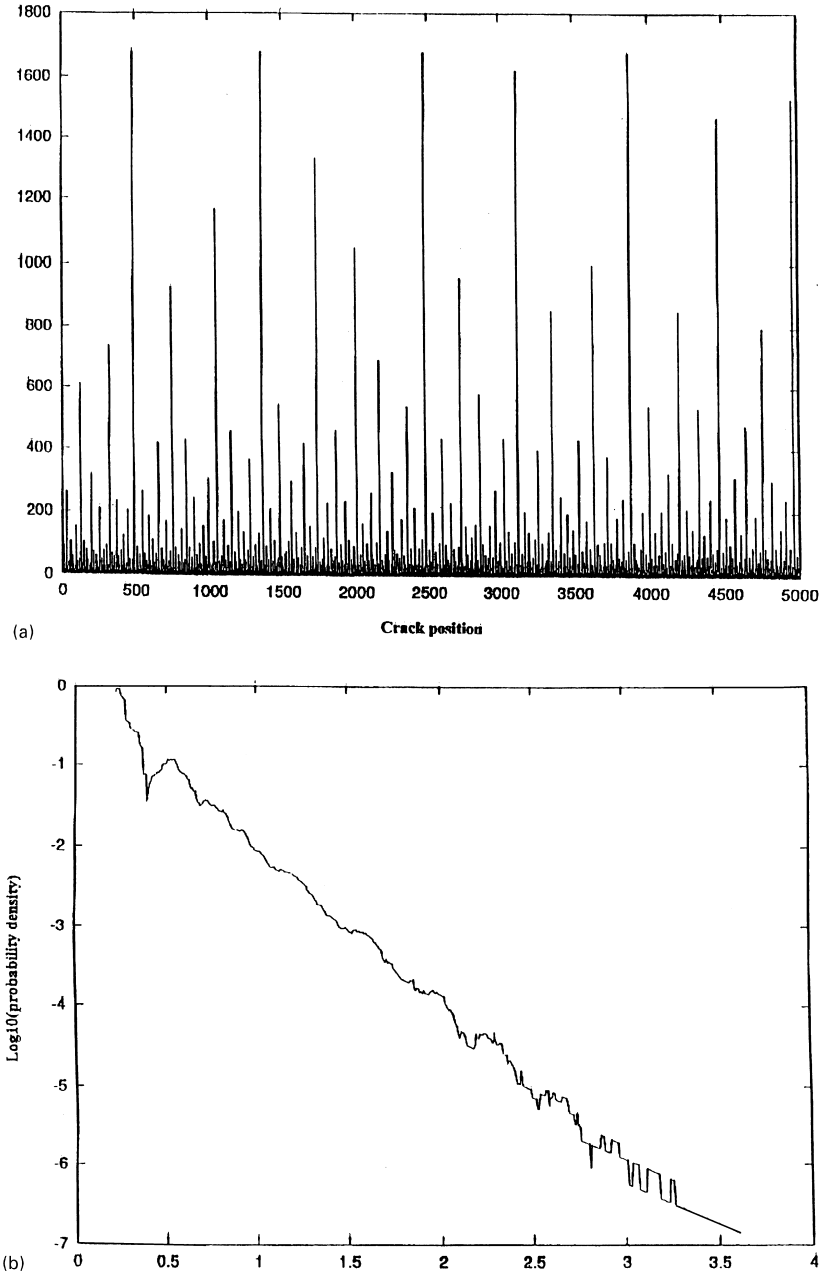

Fig. 4. (a) Map of 5000 needles which have grown according to the DLA rules from an initial configuration where all the needles were approximately of the same length equal to their average separation. We have used a periodic lattice and added a small random value (a few percent of the period) for their lateral position. This configuration corresponds to the time when the largest needle has a length equal to one-third of the size of the system. (b) The probability density function of the needle lengths shown in (a) in where very clear log-periodic oscillations decorate the power-law behavior (see Ref. [48]).

coupling between modes of growth [48]. Let us mention that, in the early 1980s, Sadovskiy et al. have argued for the existence of a discrete hierarchy in fracture and rock properties [55–59], with a preferred scaling ratio around 3.5. Borodich [60, 116–118] discusses the use of parametric-homogeneous functions for a parcimonious mathematical representation of structure presenting a hierarchy of log-periodicities.

In their theoretical analysis, Ball and Blumenfeld [62] predicted logarithmic oscillations in quasi-static crack growth, probably one of the very first example of such oscillations in non-tree structures. First, they coarse-grained a quasi-static growing crack as a wedge and found the behavior of the stress field around it. Then, they showed through a linear stability analysis that there is an instability to growth of branches where the stress is locally high. In this, it is conceptually similar to the DLA instability with respect to a locally high gradient of the field near the interface. Then they argued that because of this instability the dynamics couple to sub-dominant terms in the stress field to generate branches. So looking into what are the strongest subdominant terms, they could identify the behaviour of the branching. These terms happened to have the functional form

$$S_n = A_n r^{a_n + \mathrm{i}b_n},$$

where A_n, $a_n(<0)$, and b_n are numbers and S_n is the stress due to the contribution of the nth term in the expansion of the stress field. Their argument was that, since these terms exhibit logarithmic oscillations, then so will the branching in the cracking pattern, resulting in a growing dendrite with logarithmically periodic branches.

5.3.2. Log-periodicity in time

A growing body of evidences indicate that the log-periodic oscillations appear in the time dependence of the energy release on the approach of impending rupture in laboratory experiments [19], numerical simulations [61–63] and earthquakes [15–18, 64–66]. It is thought that a similar type of cascade, from progressive damage at small scale to coalescence and unstable growth, is controlling the appearance of log-periodicity. The typical time-to-failure formula used in these works is

$$E \sim (t_\mathrm{r} - t)^m \left[1 + C\cos\left(2\pi\frac{\log(t_\mathrm{r} - t)}{\log\lambda} + \Psi\right)\right], \tag{27}$$

where E is the energy released or some other variable quantifying the on-going damage, t_r is the time of rupture, m is a critical exponent, and Ψ is a phase in the cosine that can be get rid of by a change of time units. It has been found that the log-periodic oscillations enable a much better reliability of the prediction due to "lock-in" of the fit on the oscillating structure. Physically, the oscillations contain information on t_r and thus help significantly in its determination. A link between log-periodicity in space and in time is given in Ref. [67]. A typical fit by expression (Eq. (27)) to acoustic emission data is presented in Fig. 5.

5.4. Cascade of structure in hydrodynamics

Moffatt [142] has studied similarity solutions for the flow of a viscous fluid near a sharp corner between two plates on which a variety of boundary conditions are imposed. For this, one has to

solve the biharmonic Stokes equation for the stream function which admits separable solutions in plane polar coordinates (r,θ): $\Psi = r^{\alpha} f_{\alpha}(\theta)$. For angles between the two plates less than 146°, the exponent α has been shown to be necessarily complex [143], Moffatt has shown that this result can be interpreted as implying the existence of an infinite sequence of eddies near the corner. It is interesting that viscosity, usually a damping mechanism, is here responsible for the generation of a geometrical progression of eddies. The damping has the effect, however, to give a large ratio (typically greater than 300) of the intensities between successive eddies.

Recent experiments and analysis both numerical and analytical of droplet fission shows the existence of iterated instabilities that develop a discrete scale invariance. The reason for self-similarity is that, near breakoff, the droplet radius becomes much smaller than any other length scale, so that the shape of the interface becomes independent of these scales. Numerical simulations of the corresponding hydrodynamic equations with a weak noise source show that necks and blobs form repeatedly on smaller and smaller scales as the interface breaks [144]. These instability cascades are only observed for fluids with a viscosity greater than 1 P. The mechanism behind this cascade of instabilities is that, immediately before a neck forms, the thinnest section of the interface is well approximated by the similarity solution. The nonsteady singularity results from repeated instabilities of the similarity solution due to thermal capillary waves.

5.5. *Cascades of sub-harmonic bifurcations in the transition to chaos*

An area where log-periodic structures should be expected is low-dimensional dynamical systems exhibiting the Feigenbaum sequence of subharmonic bifurcations to chaos [68–72]. Indeed, this route to chaos can be understood from an asymptotically exact *discrete* renormalization group with a universal scaling factor. The existence of this preferred scaling ratio should thus lead to complex exponents and log-periodic oscillations around the main scaling as the dynamics converges to the invariant Cantor set measure at criticality. It was noticed quite early [73–75] that the length of the stable period diverges as a power law with log-periodic modulations as the control parameter approaches the transition to chaos. Argoul et al. [76] have studied the transitions to chaos in the presence of an external periodic field and show figures exhibiting very clearly that the Lyapunov exponent has a power dependence with log-periodic oscillations as a function of the amplitude of the external field. Similarly, the topological entropy at the onset of pruning in generalized Baker transformations is a power law function of the distance to the onset of pruning with log-periodic oscillations [78]. The oscillations are due to the self-similar structure of the Cantor set forming the attractor [73–75, 77].

5.6. *Animals*

We have noticed [8] that, in contrast to common lore, complex critical exponents should generally be expected in the field theories that describe geometrical systems, because the latter are *non-unitary*. In particular, evidence of complex exponents in lattice animals, a simple geometrical generalization of percolation has been presented [8]. The model of lattice animals is the most natural generalization of the percolation model, which itself is the prototype of disordered systems. The animal problem is the statistics of connected clusters on a lattice [79, 80] and thus also

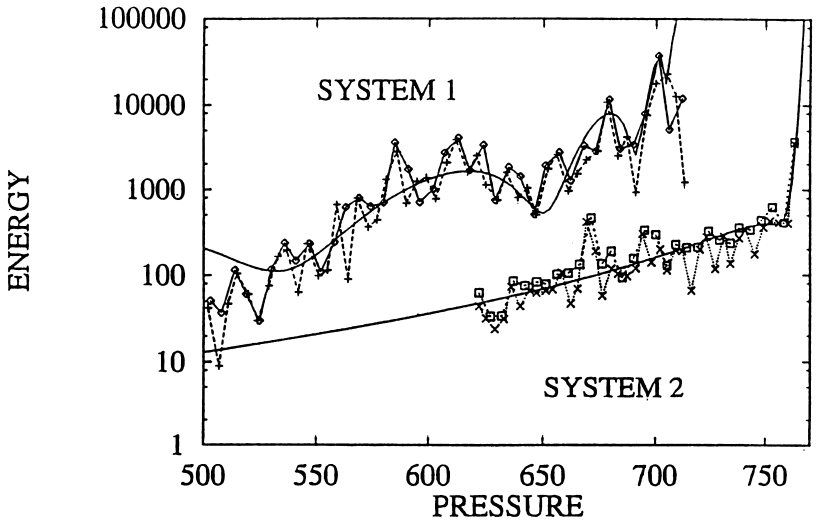

Fig. 5. Logarithm of the acoustic emission energy released as a function of the pressure (in bars) applied within a pressure tank made of matrix-fiber composite at the approach of rupture. The continuous lines correspond to the best fit by expression (Eq. (27)) (see Ref. [19]).

describes unrooted branched polymers. Using transfer matrix techniques, the number of unrooted branched polymers of size N is found to exhibit a correction to the main scaling with a complex exponent.

Recall that in the percolation problem, bonds are occupied with a probability p and unoccupied with probability $1-p$. For a given configuration, connected parts are called clusters. To study the statistics of one percolation cluster, one can sum over all configurations for the bonds that do not belong to this cluster nor to its perimeter. Since they are either occupied or inoccupied, the sum over all configurations just gives a unit weight. Hence, in percolation, clusters are simply weighed with $p^{N_b}(1-p)^{N_p}$ where N_b is the number of bonds in the cluster, N_p the number of bonds of the perimeter. Now the animal problem is a more general model where a cluster is weighed by $p^{N_b}q^{N_p}$ with general values of p, q. By varying p, q a critical point is met which is always in the same universality class of so-called animals. Only when $p+q=1$ is this critical point in a different universality class, percolation, which therefore can be considered as a tricritical point in the animals parameter space.

The result of the analysis of Ref. [8] is that the number T_N of unrooted branched polymers of size N in the plane is given by

$$T_N \approx \left(\frac{1}{p_c}\right)^N [N^{\nu(2-2X_1)-3} + cN^{\nu(2-2X_{2,R}-3)}\cos(2X_{2,I}\nu \log N + \phi)] \ , \tag{28}$$

where ν is the radius of gyration exponent, $\nu \approx 0.64$. Recall that the leading term in Eq. (28) is actually known exactly $\nu(2-2X_1)-3 = -1$ [81]. Hence, we see log-periodic terms to appear in the next to leading behavior of T_N. Unfortunately, since conformal invariance is broken, this argument does not allow us to make any predictions on the amplitude of these terms, which might

well be very small. The DLA problem is much more favorable in that respect probably due to enhancement effects stemming from the long-range interactions of Laplacian fields.

5.7. Quenched disordered systems

Renormalization group analysis of a variety of spin problems with long-ranged quenched interactions have found complex critical exponents [82–86]. However, these authors have in general remained shy as to the reality of their results. Indeed, one could argue that uncontrolled approximations (present in all these works) rather than physics could be the cause of the complex exponents. Derrida and Hilhorst have also found log-periodic corrections to the critical behavior of 1D random field Ising model at low temperature by analyzing products of random non-commutative matrices [87].

With the qualitative understanding of the ultrametric structure of the energy landscape of spin glasses [88, 89] in the mean-field approximation, one could conjecture that these above results could be the observable signature of the hierarchical structure of energy states in frozen random systems. The problem is that, even if hierarchical, the ultrametric structure is believed to be continuous and it is not clear what could produce the discrete-scale symmetry. It is generally believed that such topology occurs more generally in other complex systems with highly degenerate, locally stable states [90]. However, much works remain to be done to clarify this problem. The additional presence of long-range interactions complicate the matter further.

A dynamical model describing transitions between states in a hierarchical system of barriers modelling the energy landscape in the phase space of mean-field spin glasses leads again to log-periodic corrections to the main $\log t$ behavior [8].

Let us also mention that mth critical Ising models ($m = 1$ for the Gaussian model, $m = 2$ for Ising, $m = 3$ for tricritical Ising, etc.) have a free energy exhibiting log-periodic oscillations as a function of the control parameter for large m, a signature of the geometrical cascade of multicritical points [91–93, 8].

6. Other systems

6.1. The bronchial tree

It has been pointed out that the morphology of the bronchial airway of the mammalian lung is roughly hierarchical leading to a log–log plot of the average diameter of a branch of a mammalian lung (for human, dog, rat and hamster) as a function of the branch order which exhibits a full S-oscillation (log-periodic) decorating an average linear (power law) dependence. This fractal structure has been argued to allow the organ to be more stable with respect to disturbance [94–97] but the physical mechanism underlying its appearance is not understood.

6.2. Turbulence

Probably, the first theoretical suggestion of the relevance of log-periodic oscillations to physics has been put forward by Novikov to describe the influence of intermittency in turbulent flows [3].

The idea is that the DSI could stem from the existence of a prefered ratio in the cascade from large eddies to small ones. The existence of log-periodic oscillations has not been convincingly demonstrated as they seem quite elusive and sensitive to the global geometry of the flow and recirculation [98, 99]. Shell models of turbulence, which have attracted recently a lot of interest [100–102] construct explicitly a discrete-scale invariant set of equations. In these models, self-similar solutions of the cascade of the velocity field and energy in the discrete-log-space scale have been unravelled [103, 104], whose scaling can be related to the intermittent corrections to Kolmogorov scaling. We note that some of these solutions rely on the discrete-scaling shell structure and would disappear in the continuous limit. However, the relevance of these discrete hierarchical models and more generally of log-periodic oscillations have not been explored systematically and their confirmation in turbulence remains open.

6.3. Titius–Bode law

Dubrulle and Graner [105, 106] have noticed that the Titius–Bode law of planets distance to the sun $r_n = r_0 K^n$ with $K \approx 1.7$ can be seen a discrete-scale invariant law (K then plays the role of λ in our notation). They show that all models that have been proposed to explain the Titius–Bode law share the common ingredient of scale symmetry. Assuming a discrete symmetry breaking in the rotation invariance, they thus show that any such mechanism is compatible with the Titius–Bode law. As a consequence, this law cannot a priori be used to constraint the mechanism of planet formation and their organization around the sun. What is however not understood is the physical mechanism, if any, at the basis of the breakdown of continuous to discrete scale invariance embodied in the Titius–Bode law.

6.4. Gravitational collapse and black-hole formation

Choptuik [107] has recently shown that, in contrast to the general view, black holes of mass smaller than the Chandrasekar limit could be formed and that, in the process of formation, the solutions would oscillate periodically in the logarithm of the difference between time and time of the formation of the singularity. This gravitational collapse is an example of critical behavior, describing how the mass M of the black hole depends on the strength p of the initial conditions: $M \sim (p - p^*)^\gamma$ for $p > p^*$ and 0 otherwise, where p^* is the threshold value. It has been shown that classical close-to-critical black holes (obeying Einstein's equations) coupled to a massless complex scalar field have a leading real exponent γ_R and a subleading complex exponent [107–110], which would correspond to a log-periodic spectrum of masses. Alternatively, the real and complex exponents control the time development of the black-hole instability which is also log-periodic in time, corresponding to continuous-phase oscillations of the field.

6.5. Rate of escape from stable attractors

Let us also mention the recently discovered log-periodic behavior of the rate of escape from a stable attractor surrounded by an instable limit cycle as a function of the strength of the white

noise [111]. This is an example where the rate of escape, as calculated from a Fokker–Planck equation, is non-Arhenius.

6.6. Interface crack tip stress singularity

Complex singularities are also found in the divergence of the stress as a function of the distance to the tip of a crack at the interface between two different elastic media [112]. The standard $\sigma \sim r^{-1/2}$ singularity, where r is the distance to the crack tip and σ is the stress, is replaced by

$$\sigma \sim r^{-(1/2)+i\omega}, \tag{29}$$

where

$$\omega = \frac{1}{2\pi}\log\left(\frac{\dfrac{\kappa_1}{\mu_1}+\dfrac{1}{\mu_2}}{\dfrac{\kappa_2}{\mu_2}+\dfrac{1}{\mu_1}}\right). \tag{30}$$

Subscripts 1 and 2 refer to the material in $y > 0$ and $y < 0$, respectively; $\kappa = 3 - 4\nu$ for plane strain and $\kappa = (3-\nu)/(1+\nu)$ for plane stress, ν is the Poisson ratio and μ is the shear modulus. Interface cracks have important practical applications since interfaces between composite media are often the locii of damage nucleation leading to the incipient rupture. The existence of this complex singularity suggests that the mechanism of damage and rupture at interfaces could be quite different from that in the bulk [113]. Following this work, a wealth of studies have followed (see Refs. [113, 114] and references therein), but the physical understanding of the appearance of a complex critical singularity has remained elusive. Since the solution shows that the two modes of deformations in tension and shear (modes I and II) are intrinsically coupled for an interface crack in contrast to what happens for a crack in an homogeneous medium, one could hope to identify the physical origin of the complex exponent in this coupling. Let us also mention that the pressure distribution as a function of distance to the corner in the Hertz problem of two different elastic spheres compressed against each other is also described by a power law with complex exponent [115].

6.7. Eigenfunctions of the Laplace transform

Log-periodicity and complex exponents play a very important role in integral equations of the type $g(\tau) = \int_0^\infty K(v\tau)p(v)\,dv$, with $0 \le \tau < \infty$ where the kernel K has the property $\int_0^\infty |K(x)|x^{-1/2}\,dx < \infty$. This class of equation includes the Laplace transform, the Fourier sine and cosine transforms and many other integral equations of importance in physics. It is notorious that the inversion problem of getting $p(v)$ from the measurement of $g(\tau)$ is ill-conditioned. This can be seen to result from the form of the eigenfunctions and eigenvalues of the Laplace transform and similar dilationally invariant Fredholm integral equation [120]. For instance, the eigenfunctions of the Laplace transform, which form a complete orthogonal basis, are $\phi_\omega^+(v) = v^{-1/2}\cos(\omega \ln v - \theta_\omega)$ and $\phi_\omega^-(v) = -v^{-1/2}\sin(\omega \ln v - \theta_\omega)$, where θ_ω is a function of ω. The eigenvalues are exponentially decreasing with ω and this controls the ill-conditioned nature of the Laplace inversion. The log-periodicity of the eigenfunctions lead to an optimal sampling determined by a generalized Shannon theorem which obeys a geometrical series [121].

7. Applications

7.1. Identifying characteristic scales

In our opinion, the main interest in identifying log-periodicity in data is the characterization of the characteristic scales associated to it. Indeed, it must be clear that the log-periodic corrections to scaling imply the existence of a hierarchy of characteristic scales (in space or time). For instance, in the time-to-failure analysis given by Eq. (27), the hierarchy of time scales is determined by the local positive maxima of the function E. They are given by

$$t_r - t_n = \tau\lambda^{n/2}\,, \tag{31}$$

where $\tau \propto \exp(-(\log\lambda/2\pi)\tan^{-1}(2\pi/m\log\lambda))$. The spacing between successive values of t_n approaches zero as n becomes large and t_n converges to t_r. This hierarchy of scales $t_r - t_n$ are not universal but depend upon the specific geometry and structure of the system. What is expected to be universal are the ratios $(t_r - t_{n+1})/(t_r - t_n) = \lambda^{1/2}$. From three successive observed values of t_n, say t_n, t_{n+1} and t_{n+2}, we have

$$t_r = \frac{t_{n+1}^2 - t_{n+2}t_n}{2t_{n+1} - t_n - t_{n+2}}\,. \tag{32}$$

This relation is invariant with respect to an arbitrary translation in time. In addition, the next time t_{n+3} is predicted from the first three ones by

$$t_{n+3} = \frac{t_{n+1}^2 + t_{n+2}^2 - t_n t_{n+2} - t_{n+1}t_{n+2}}{t_{n+1} - t_n}\,. \tag{33}$$

These relations have been used in Refs. [34, 18, 64]. Physically, time or space scales give us access to additional information and clues about the underlying processes and the existence of a hierarchy of preferred scales, as in DSI, will tell us something about the underlying processes. This is lost in usual critical behavior in which all scales are treated as playing the same role.

7.2. Time-to-failure analysis

Another important application of log-periodicity is its use in making more robust and precise time-to-failure analysis. We have already mentioned the importance of log-periodicity for predictions [15–22]. The derived time-to-failure analysis is now being implemented for routine industrial testing in the space industry in Europe. As already mentioned, the reason for this improvement is that a fit can "lock-in" on the oscillations which contain the information on the time of failure and thus lead to a better prediction.

7.3. Log-periodic antennas

Let us mention the engineering application of antennas using log-periodic electromagnetic antennas [122–128]. The DSI structure provides an optimal compromise between maximizing bandwidth and radiation efficiency.

7.4. Optical waveguides

Graded-index optical waveguides with optimized index profiles can support a family of weakly localized modes with algebraic tails with log-periodic modulations in the evanescent field [119]. The log-periodic oscillations result from an interplay between the critical nature of the modes and absorption (complex index of refraction). This could have applications in techniques using evanescent waves.

8. Open problems

8.1. Non-linear map and multicriticality

In this brief review, we have kept the analysis of the renormalization group at the level of a linear expansion of the flow map. Taking into account the non-linear structure of the flow map, as for instance in Eq. (14), may lead to an infinite set of singularities accumulating at the main critical point or even to the whole axis of the control parameter being critical (in the chaos regime of the flow map [129]). The question of the relevance of these regimes to nature is still open (see Ref. [16] for a proposed application to earthquakes). Generalization to several control parameters and multicritical points would be useful.

8.2. Multilacunarity and quasi-log-periodicity

We have seen that DSI embodies the concept of lacunarity. The set of complex exponents or singularities has been called *multilacunarity* spectrum [25]. Generalizations with several different incommensurate log-frequencies would be of great interest and seem to appear, for instance, in the DLA problem [11]. Complex multifractal dimension spectrum in the presence of disorder can be handled using probabilistic versions of the renormalization group [130] and their development and impact are just emerging. Note also that the set of complex exponents provides a better characterization of the underlying multiplicative process and could improve the conditioning of the inverse fractal problem [131]. The q-derivative is a natural tool to discuss homogeneous functions with oscillatory amplitudes. It has recently been used to describe cascade and multifractal models with continuous-scale changes [132].

8.3. Effect of disorder

A very important practical question is the effect of disorder and the process of averaging. Disorder is expected to scramble the phases of the log-periodic oscillations and it is a priori not clear whether the log-periodic oscillations are robust. It turns out that small fluctuations around the log-periodic structure do not seem to spoil DSI, as found in many examples quoted above. For instance, in the needle DLA problem, intervals between needles were taken to fluctuate by a few percent without altering significantly the log-periodic structure of the growth process [48]. DLA clusters themselves are formed under a very strong annealed noise, corresponding to the random walk motion of the sticking particles. Nevertheless, clear evidence of log-periodicity in the mass as

a function of radius has been found [11] giving confidence in their robustness with respect to disorder. This has been further substantiated by explicit calculations [8] showing generally that the complex exponents are robust.

8.4. Averaging: Grand canonical versus canonical

However, we must stress that disorder introduces a sensitive dependence of the phase in the cos log formula: different realizations have a different phase and averaging will produce a "destructive interference" that makes vanish the log-periodic oscillations. It is thus important to carry out analysis on each sample realization separately, *without* averaging. For instance, in the DLA case, 350 clusters of 10^6 particles have each been analyzed one by one and an histogram of the main log-frequencies has been constructed. Theoretically, preventing averaging is a problem as one is usually able only to calculate quantities averaged over the different realizations of the disorder. However, it must be stressed that the fact that log-periodic oscillations are mainly present before averaging tells us that they are *specific* fingerprints of the specific system one is looking at. This is obviously a desirable property for prediction purposes in engineering and other practical applications. An open problem however is to devise optimal tools to decipher the log-periodic structures in highly noisy data, as is usually the case due to limitation of sizes for instance. We note also that going to very large systems will in general progressively destroy the log-periodic structures as they are often correction to scaling.[9] Random versions of Cantor fractal sets have recently been shown to exhibit robust log-periodic structures even when averaging [133].

Pazmandi et al. [136] have recently argued that the standard method of averaging carried out in disordered systems introduces a spurious noise of relative amplitude proportional to the inverse square root of the system size. This so-called "grand canonical" averaging can thus destroy more subtle fluctuations in finite systems, controlled by a correlation length exponent less than $2/d$ ($2/d$ is the minimum value of the correlation length exponent that would not be hidden by the usual grand canonical averaging). Pazmandi et al. thus propose an alternative averaging procedure, the so-called "canonical" averaging, which consists in identifying, for each realization, the corresponding specific value of the critical control parameter K_c^R. The natural control parameter then becomes $\Delta = (K - K_c^R)/K_c^R$ and the act of averaging can then be performed for the samples with the same Δ. We have used this procedure to identify log-periodicity in the elastic energy E prior to rupture in a dynamical model of rupture in heterogeneous media. Previous works have shown that E follows a power law $E \sim (t_r - t)^{-\alpha}$ as a function of the time to failure [137–140]. Performing the usual (grand canonical) averaging over twenty different realizations of the disorder provides very good evidence of the power law but no evidence of log-periodicity. We have thus developed the following alternative averaging procedure [141]. We constructed the second derivative of E with respect to time for each realization, thinking of it as a kind of susceptibility. The time t_r^R at which this second derivative is maximum has been identified and this point has been used as the effective value of the

[9] This is often due to the disorder which can be shown to renormalize the real part of the complex exponents so that they correspond to sub-leading correction to the main scaling behavior [8, 11].

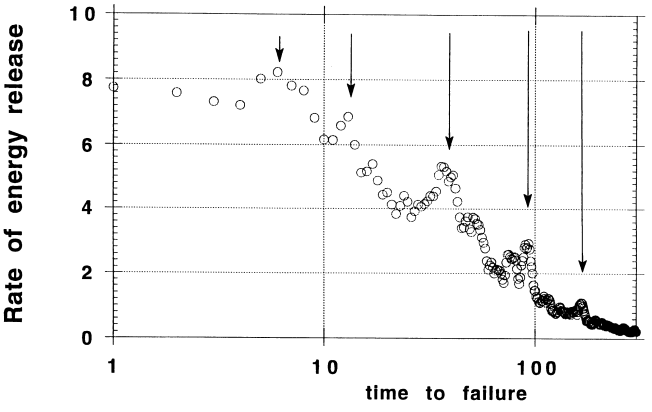

Fig. 6. Rate of elastic energy released as a function of the logarithm of the time to failure in the dynamical model of rupture with damage introduced in Ref. [137]. The dots have been obtained using the "canonical" averaging procedure discussed in the text.

time t_r of rupture for each realization. Then, the first derivative, giving the rate of energy released, is averaged over all samples with the same $(t_r^R - t)/t_r^R$. The result is presented in Fig. 6 in a log–log scale. Four to five approximately equidistant spikes (in log scale) are clearly visible. The log-period allows us to identify a preferred scaling ratio $\lambda = 2.5 \pm 0.3$. It is probable that similar averaging procedures better tailored to get rid of spurious fluctuations from realization to realization will play an increasing role in the physics of disordered and turbulent media.

8.5. Amplitude of log-periodicity

Log-periodicity is found in spin systems in hierarchical lattices. However, the effect is usually very small, typically 10^{-4} or less in relative amplitude. In contrast, we have found it much stronger in rupture and growth process, typically 10^{-1} or so in relative amplitude. The reason is not very well understood but might stem from the strong amplification effects occurring in such Laplacian fields.

8.6. Where to look for log-periodicity

From the point of view of non-unitary field theory, we should expect generically the existence of complex exponents. However, there is no known recipe to tell us what are the relevant observables that will have complex dimensions. Practically, this means that it is not a priori obvious what measure must be made to identify log-periodicity. In other words, it is important to look carefully at the available data in all imaginable angles to extract the useful information. Of course, one must always be aware of statistical traps that noise can be taken for log-periodicity. Analysis must thus be carried out with synthetic tests for the null hypothesis, bootstrap approach, etc. (see for instance Refs. [18, 48] for the application of statistical tests and the bootstrap method in this context).

8.7. Preferred scaling ratio around 2?

Another puzzling observation is the value of the preferred ratio $\lambda \approx 2$, found for a wide variety of systems, such as in growth processes, rupture, earthquakes, and financial crashes. H. Saleur (private communication) has noticed that 2 is in fact the mean-field value of λ obtained by taking an Ising or Potts model (with Q states) on a hierarchical lattice in the limit of an infinite number of neighbors. Consider a diamond lattice with n bonds connected to the upper and lower nodes (the usual diamond lattice discussed above has $n = 2$). The discrete renormalization group equation connecting $K = e^{\beta J}$, where β is the inverse temperature and J the coupling coefficient, from one generation to the next is the generalized version of Eq. (14) to n-bonds connectivity:

$$K'(K) = [f(K)]^n = \left(\frac{K^2 + Q - 1}{2K + Q - 2}\right)^n . \tag{34}$$

In the limit $n \to \infty$ where the number of coupled nodes increases without bounds, we expect physically the ordered–disordered transition to occur at larger and larger temperature, corresponding to a fixed point of Eq. (34) $K'(K^*) = K^* \to 1$. Expanding around 1, we indeed find $K^* = 1 + Q/n$ asymptotically. The linearization of the renormalization group map (Eq. (34)) gives $K' - K^* = \lambda(K - K^*)$ with $\lambda = nK^* \, \mathrm{d} \log f/\mathrm{d}K|_{K^*} \to 2$ in the limit $n \to \infty$. Can this argument be extrapolated to out-of-equilibrium systems?

8.8. Critical behavior and self-organized criticality

Time-to-failure analysis of earthquakes seem at variance with the globally stationary viewpoint, for instance captured by the concept of self-organized criticality as applied to plate tectonics [134, 135]. Recently, it has been shown [67] that a simple model of earthquakes on a pre-existing hierarchical fault structure exhibits both self-organization at large times in a stationary state with a power-law Gutenberg–Richter distribution of earthquake sizes. In the same token, the largest fault carries irregular great earthquakes preceded by precursors developing over long time scales and followed by aftershocks obeying the $1/t$ Omori's law of the rate of seismicity after a large earthquake. The cumulative energy released by precursors follows a time-to-failure power law with log-periodic structures, qualifying a large event as an effective dynamical (depinning) critical point. Down the hierarchy, smaller earthquakes exhibit the same phenomenology, albeit with increasing irregularities. The robustness of this scenario for other models and situations is currently being studied.

Acknowledgements

I wish to thank my collaborators J.-C. Anifrani (Bordeaux, France), A. Arneodo (Bordeaux, France), J.-P. Bouchaud (Saclay, France), Y. Huang (USC, Los Angeles), C. Le Floc'h (Bordeaux, France), J.-F. Muzy (Bordeaux, France), W.I. Newman (UCLA, Los Angeles), G. Ouillon (Nice, France), C. Sammis (USC, Los Angeles), B. Souillard (Orsay, France), U. Tsunogai (Tokyo, Japan), C. Vanneste (Nice, France), H. Wakita (Tokyo, Japan), who participated on diverse parts of this work. A special mention should be made to A. Johansen (Copenhagen, Denmark) and H. Saleur

(USC, Los Angeles). I am also grateful to A. Johansen for a critical reading of the manuscript. This is publication 4901 of the Institute of Geophysics and Planetary Physics at UCLA.

References

[1] B.B. Mandelbrot, The Fractal Geometry of Nature, W.H. Freeman, San Francisco, 1982.
[2] G.A. Edgar (Ed.), Classics on Fractals, Addison-Wesley, Readings, MA, 1993.
[3] E.A. Novikov, Dokl. Akad. Nauk SSSR 168/6, 1279 (1966).
[4] E.A. Novikov, Phys. Fluids A 2 (1990) 814.
[5] G. Jona-Lasinio, Nuovo Cimento 26B (1975) 99.
[6] M. Nauenberg, J. Phys. A 8 (1975) 925.
[7] Th. Niemeijer, J.M.J. van Leeuwen, in: C. Domb, M.S. Green (Eds.), Phase Transitions and Critical Phenomena, vol. 6, Academic Press, London, 1976, p. 425.
[8] H. Saleur, D. Sornette, J. Phys. I France 6 (1996) 327.
[9] P. Bak, How Nature Works: the Science of Self-organized Criticality, Copernicus, New York, NY, USA, 1996.
[10] D.J. Wallace, R.K.P. Zia, Phys. Lett. 48A (1974) 325.
[11] D. Sornette, A. Johansen, A. Arnéodo, J.-F. Muzy, H. Saleur, Phys. Rev. Lett. 76 (1996) 251.
[12] J. Cardy, J. Phys. A 17 (1984) L385.
[13] S. Weinberg, preprint hep-th/9702027.
[14] S. Weinberg, The Quantum Theory of Fields, Cambridge University Press, Cambridge, 1995.
[15] D. Sornette, C.G. Sammis, J. Phys. I France 5 (1995) 607.
[16] H. Saleur, C.G. Sammis, D. Sornette, Nonlinear Processes Geophys. 3 (2) (1996) 102.
[17] H. Saleur, C.G. Sammis, D. Sornette, J. Geophys. Res. 101 (1996) 17661.
[18] A. Johansen, D. Sornette, H. Wakita, U. Tsunogai, W.I. Newman, H. Saleur, Japan, J. Phys. I France 6 (1996) 1391.
[19] J.-C. Anifrani, C. Le Floc'h, D. Sornette, B. Souillard, J. Phys. I France 5 (6) (1995) 631.
[20] J.-C. Anifrani, A. Johansen, C. Le Floc'h, G. Ouillon, D. Sornette, C. Vanneste, B. Souillard, Proc. 6th European Conf. on Non-Destructive Testing, 24–28 October 1994, Nice, Presentation N72.
[21] D. Sornette, A. Johansen, J.-P. Bouchaud, J. Phys. I France 6 (1996) 167.
[22] J.A. Feigenbaum, P.G.O. Freund, Int. J. Mod. Phys. 10 (27) (1996) 3737.
[23] D. Sornette, A. Johansen, Physica A 245 (1997) 411.
[24] D. Bessis, J.-D. Fournier, G. Servizi, G. Tourchetti, S. Vaienti, Phys. Rev. A 36 (1987) 920.
[25] J.-D. Fournier, G. Tourchetti, S. Vaienti, Phys. Lett. A 140 (1989) 331.
[26] E. Orlandini, M.C. Tesi, G. Turchetti, Europhys. Lett. 21 (1993) 719.
[27] A. Kapitulnik, A. Aharony, G. Deutscher, D. Stauffer, J. Phys. A 16 (1983) L269.
[28] M.O. Vlad, M.C. Mackey, Phys. Scripta 50 (1994) 615.
[29] D. Bessis, J.S. Geronimo, P. Moussa, J. Phys. Lett. 44 (1983) L977.
[30] B. Douçot, W. Wang, J. Chaussy, B. Pannetier, R. Rammal, Phys. Rev. Lett. 57 (1986) 1235.
[31] B. Derrida, L. De Seze, C. Itzykson, J. Stat. Phys. 33 (1983) 559.
[32] B. Derrida, C. Itzykson, J.M. Luck, Commun. Math. Phys. 94 (1984) 115.
[33] Y. Meurice, G. Ordaz, V.G.J. Rodgers, Phys. Rev. Lett. 75 (1995) 4555.
[34] W.I. Newman, D.L. Turcotte, A.M. Gabrielov, Phys. Rev. E 52 (1995) 4827.
[35] B. Kutjnak-Urbanc, S. Zapperi, S. Milošević, H.E. Stanley, Phys. Rev. E 54 (1996) 272.
[36] D. Karevski, L. Turban, J. Phys. A 29 (1996) 3461.
[37] F.Y. Wu, Rev. Mod. Phys. 54 (1982) 235.
[38] P. Flajolet, M. Golin, in: A. Lingas, R. Karlsson, S. Carlsson (Eds.), Automata, Languages and Programming, 20th Int. Coll., ICALP 93 Proc. Springer, Berlin, 1993, pp. 137–149.
[39] P. Flajolet, P. Grabner, P. Kirschenhofer, H. Prodinger, R.F. Tichy, Theoret. Comput. Sci. 123 (1994) 291.
[40] J. Bernasconi, W.R. Schneider, J. Phys. A 15 (1983) L729.

[41] M.O. Vlad, Int. J. Mod. Phys. B 6 (1992) 417.
[42] M.O. Vlad, J. Phys. A 25 (1992) 749.
[43] D. Dee, M. Ghil, SIAM J. Appl. Math. 44 (1984) 111.
[44] M. Ghil, A. Mullhaupt, J. Stat. Phys. 41 (1985) 125.
[45] A. Arneodo, F. Argoul, E. Bacry, J.F. Muzy, Phys. Rev. Lett. 68 (1992) 3456.
[46] A. Arneodo, F. Argoul, J.F. Muzy, M. Tabard, Phys. Lett. A 171 (1992) 31.
[47] A. Arneodo, F. Argoul, J.F. Muzy, M. Tabard, E. Bacry, Fractals 1 (1993) 629.
[48] Y. Huang, G. Ouillon, H. Saleur, D. Sornette, Phys. Rev. E 55 (1997) 6433.
[49] G. Ouillon, D. Sornette, A. Genter, C. Castaing, J. Phys. I France 6 (1996) 1127.
[50] J.M. DeGraff, A. Aydin, JGR 98 (B4) (1993) 6411.
[51] D.D. Pollard, A. Aydin, Geol. Soc. Am. Bull. 100 (1988) 1181.
[52] S. Nemat-Nasser, L.M. Keer, K.S. Parihar, Technical Report No. 77-9-2, Earthquake Research and Engineering lab., Department of Civil Engineering, Northwestern University, September 1977.
[53] S. Nemat-Nasser, L.M. Keer, K.S. Parihar, Int. J. Solids Struct. 14 (1978) 409.
[54] S. Nemat-Nasser, A. Oranratnachai, Trans. ASME 101 (1979) 34.
[55] M.A. Sadovskiy, Dokl. Akad. Nauk SSSR, 247 (4) (1979) 829.
[56] M.A. Sadovskiy, L.G. Bolkhovitinov, V.F. Pisarenko, Izv. Akad. Nauk SSSR Fizika Zemli 12 (1982) 3.
[57] M.A. Sadovskiy, V.F. Pisarenko, Inst. Fiz. Zemli Akad. Nauk SSSR 2 (1982).
[58] M.A. Sadovskiy, V.F. Pisarenko, V.N. Rodionov, Vestn. Akad. Nauk SSSR 1 (1983) 82.
[59] M.A. Sadovskiy, T.V. Golubeva, V.F. Pisarenko, M.G. Shnirman, Izv. Earth Phys. 20 (1984) 87.
[60] F.M. Borodich, J. Mech. Phys. Solids 45 (1997) 239.
[61] M. Sahimi, S. Arbabi, Phys. Rev. Lett. 77 (1996) 3689.
[62] R.C. Ball, R. Blumenfeld, Phys. Rev. Lett. 65 (1990) 1784.
[63] R.C. Ball, R. Blumenfeld, Phys. Rev. Lett. 68 (1992) 2254.
[64] D.J. Varnes, C.G. Bufe, Geophys. J. Int. 124 (1996) 149.
[65] D.D. Bowman, C.G. Sammis, EOS Trans. Am. Geophys. 77 (1996) 486.
[66] S.W. Smith, C.G. Sammis, EOS Trans. Am. Geophys. U. 77 (1996) F480.
[67] Y. Huang, H. Saleur, C.G. Sammis, D. Sornette, Europhys. Lett., in press; cond-mat/9612065.
[68] M.J. Feigenbaum, J. Stat. Phys. 19 (1978) 25.
[69] M.J. Feigenbaum, J. Stat. Phys. 21 (1979) 669.
[70] P. Coullet, C. Tresser, J. Phys. Coll. 39 (1978) C5.
[71] P. Coullet, C. Tresser, C.R. Acad. Sci. 287 (1978) 577.
[72] P. Collet, J.P. Eckmann, Iterated Maps of the Interval and Dynamical Systems, Birkhauser, Boston, 1980.
[73] B. Derrida, J. Phys. Colloques C5 (1978) 49.
[74] B. Derrida, A. Gervois, Y. Pomeau, Ann. Inst. H. Poincaré AXXIX (1978) 305.
[75] B. Derrida, A. Gervois, Y. Pomeau, J. Phys. A 12 (1979) 269.
[76] F. Argoul, A. Arnéodo, P. Collet, A. Lesne, Europhys. Lett. 3 (1987) 643.
[77] B.J. West, X. Fan, Fractals 1 (1993) 21.
[78] J. Vollmer, W. Breymann, Europhys. Lett. 27 (1994) 23.
[79] T.C. Lubensky, J. Isaacson, Phys. Rev. Lett. 41 (1978) 829.
[80] D. Stauffer, A. Aharony, Introduction to Percolation Theory, 2nd ed., Taylor and Francis, London, 1992.
[81] G. Parisi, N. Sourlas, Phys. Rev. Lett. 46 (1981) 453.
[82] A. Aharony, Phys. Rev. B 12 (1975) 1049.
[83] J.-H. Chen, T.C. Lubensky, Phys. Rev. B 16 (1977) 2106.
[84] D.E. Khmelnitskii, Phys. Lett. A 67 (1978) 59.
[85] D. Boyanovsky, J.L. Cardy, Phys. Rev. B 26 (1982) 154.
[86] A. Weinrib, B.I. Halperin, Phys. Rev. B 27 (1983) 413.
[87] B. Derrida, H. Hilhorst, J. Phys. A 16 (1983) 2641.
[88] M. Mézard, G. Parisi, M.A. Virasoro, Spin Glass Theory and Beyond, World Scientific, Singapore, 1987.
[89] R. Rammal, G. Toulouse, M.A. Virasoro, Rev. Mod. Phys. 58 (1986) 765.
[90] D.L. Stein, in: J. Souletie, J. Vannimenus, R. Stora (Eds.), Chance and Matter, North-Holland, Amsterdam, 1987.
[91] M. Lässig, Phys. Lett. B 278 (1992) 439.

[92] M. Lässig, Nucl. Phys. B 380 (1992) 601.
[93] A.W.W. Ludwig, Nucl. Phys. B 330 (1990) 639.
[94] B.J. West, Int. J. Mod. Phys. B 4 (1990) 1629.
[95] B.J. West, Ann. Biomed. Eng. 18 (1990) 135.
[96] M.F. Schlesinger, B.J. West, Phys. Rev. Lett. 67 (1991) 2106.
[97] B.J. West, W. Deering, Phys. Rep. 246 (1994) 1.
[98] F. Anselmet, Y. Gagne, E.J. Hopfinger, R.A. Antonia, J. Fluid Mech. 140 (1984) 63.
[99] U. Frisch, Turbulence, the Legacy of A.N. Kolmogorov, Cambridge University Press, Cambridge, 1995, pp. 130–131.
[100] M. Yamada, K. Okhitani, Phys. Rev. Lett. 60 (1988) 983.
[101] K. Okhitani, M. Yamada, Prog. Theor. Phys. 81 (1989) 329.
[102] M.H. Jensen, G. Paladin, A. Vulpiani, Phys. Rev. A 43 (1991) 7798.
[103] T. Nakano, Prog. Theor. Phys. 79 (1988) 569.
[104] T. Dombre, J.-L. Gilson, preprint, October 1995.
[105] F. Graner, B. Dubrulle, Astron. Astrophys. 282 (1994) 262.
[106] F. Graner, B. Dubrulle, Astron. Astrophys. 282 (1994) 269.
[107] M.W. Choptuik, Phys. Rev. Lett. 70 (1993) 9.
[108] A.M. Abrahams, C.R. Evans, Phys. Rev. Lett. 70 (1993) 2980.
[109] A.M. Abrahams, C.R. Evans, General Relativity Gravitation 26 (1994) 379.
[110] E.W. Hirschmann, D.M. Eardley, Phys. Rev. D 52 (1995) 5850.
[111] R.S. Maier, D.L. Stein, Phys. Rev. Lett. 777 (1996) 4860.
[112] M.L. Williams, Bull. Seismol. Soc. Am. 49 (1959) 199.
[113] J.R. Rice, Trans. ASME 55 (1988) 98.
[114] J.R. Rice, Z. Suo, J.-S. Wang, in: M. Ruhle, A.G. Evans, M.F. Ashby, J.P. Hirth (Eds.), Metal–Ceramic Interfaces, Acta-Scripta Metallurgica Proc. Ser., vol. 4, Pergamon Press, Oxford, 1990, pp. 269–294.
[115] K.L. Johnson, Contact Mechanics, Cambridge University Press, Cambridge, UK, 1985, p. 108.
[116] F.M. Borodich, Int. J. Solids Struct. 30 (1993) 1513.
[117] F.M. Borodich, PMM J. Appl. Math. Mech. 56 (1992) 681.
[118] F.M. Borodich, Comptes Rendus Acad. Sci. Paris II 316 (1993) 281.
[119] K. Hayata, M. Koshiba, Opt. Rev. 2 (1995) 331.
[120] J.G. McWhirter, E.R. Pike, J. Phys. A 11 (1978) 1729.
[121] N. Ostrowsky, D. Sornette, P. Parker, E.R. Pike, Opt. Acta 28 (1981) 1059.
[122] C.E. Smith (Ed.), Log Periodic Antenna Design Handbook, 1st ed., Smith Electronics, Cleveland, OH, 1966 (1979 printing).
[123] D.C. Baker, T.G. Reuss, IEEE Trans.- Broadcasting 36 (1990) 89.
[124] D.R. Dykaar, B.I. Greene, J.F. Federici, A.F.J. Levi et al., Appl. Phys. Lett. 59 (1991) 262.
[125] H.K. Smith, P.E. Mayes, IEEE Trans. Antennas Propagation 39 (1991) 1659.
[126] P.S. Excell, N.N. Jackson, K.T. Wong, IEE Proc. H Microwaves Antennas and Propagation 140 (1993) 101.
[127] R.R. Delyser, D.C. Chang, E.F. Kuester, Int. J. Microwave Millimeter-Wave Computer-Aided Eng. 3 (1993) 143.
[128] M.M. Gitin, F.W. Wise, G. Arjavalingam, Y. Pastol et al., IEEE Trans. Antennas Propagation 42 (1994) 335.
[129] B. Derrida, J.P. Eckmann, A. Erzan, J. Phys. A 16 (1983) 893.
[130] K.J. Falconer, J. Theoret. Probab. 7 (1994) 681.
[131] M.F. Barnsley, Fractals Everywhere, 2nd ed. (rev. with the assistance of Hawley Rising III), Academic Press Professional, Boston, 1993.
[132] A. Erzan, J.-P. Eckmann, Phys. Rev. Lett. 78 (1997) 3245.
[133] F.J. Solis, L. Tao, Phys. Lett. A 228 (1997) 351.
[134] A. Sornette, D. Sornette, Europhys. Lett. 9 (1989) 197.
[135] D. Sornette, Ph. Davy, A. Sornette, J. Geophys. Res. 95 (1990) 17353.
[136] F. Pazmandi, R.T. Scalettar, G.T. Zimanyi, preprint cond-mat/9704155.
[137] D. Sornette, C. Vanneste, Phys. Rev. Lett. 68 (1992) 612.
[138] D. Sornette, C. Vanneste, L. Knopoff, Phys. Rev. A 45 (1992) 8351.
[139] C. Vanneste, D. Sornette, J. Phys. I France 2 (1992) 1621.

[140] L. Lamaignère, F. Carmona, D. Sornette, Phys. Rev. Lett. 77 (1996) 2738.
[141] A. Johansen, D. Sornette, preprint 1997.
[142] H.K. Moffatt, J. Fluid Mech. 18 (1964) 1.
[143] W.R. Dean, P.E. Montagnon, Proc. Cambridge Phil. Soc. 45 (1949) 389.
[144] M.P. Brenner, X.D. Shi, S.R. Nagel, Phys. Rev. Lett. 73 (1994) 3391; X.D. Shi, M.P. Brenner, S.R. Nagel, Science 265 (1994) 219.
[145] D. Stauffer, D. Sornette, Physica A, in press; preprint cond-mat/9712085.